

Title:

**Characterizing Transport Current Defects in
1-cm-Wide $\text{YBa}_2\text{Cu}_3\text{O}_{7-\delta}$ Coated Conductors**

Author(s):

G.W. Brown, M.E. Hawley, E.J. Peterson, J.Y.
Coulter, P.C. Dowden, P.N. Arendt, S.R. Foltyn,
and F.M. Mueller

Submitted to:

<http://lib-www.lanl.gov/la-pubs/00796504.pdf>

Characterizing Transport Current Defects in 1-cm-Wide $\text{YBa}_2\text{Cu}_3\text{O}_{7-\delta}$ Coated Conductors

G.W. Brown^a, M.E. Hawley^a, E.J. Peterson^b, J.Y. Coulter^b, P.C. Dowden^b, P.N. Arendt^b, S.R. Foltyn^b, and F.M. Mueller^b

^aStructure/Property Relations (MST-8)

^bSuperconductivity Technology Center (MST-STC)

Materials Science & Technology Division,

Los Alamos National Laboratory, Los Alamos, NM 87545

ABSTRACT

We have used a low temperature magnetic imaging system to determine current pathways in 5 cm long “good” and “bad” regions of a 1-cm-wide $\text{YBa}_2\text{Cu}_3\text{O}_{7-\delta}$ coated conductor. The good and bad regions were identified with 4 point probe measurements taken at 1 cm intervals along the tape length. The current density map from the good region showed the expected edge peaked structure, similar to that seen in previous work on high quality test samples grown on single crystal substrates. The structure was also consistent with theoretical understanding of thin film superconductors where demagnetizing effects are strong. The maps from the bad region showed that the current was primarily confined to the right half of the sample. The left half carried only a small current that reached saturation quickly. Effectively halving the sample width quantitatively explains the critical current measured in that section. Spatially resolved x-ray analysis with 1 mm resolution was used to further characterize the bad section and suggested an abnormally large amount of *a*-axis YBCO present. This may be the result of non-uniform heating leading to a low deposition temperature in that area.

INTRODUCTION

An important aspect of $\text{YBa}_2\text{Cu}_3\text{O}_{7-\delta}$ coated conductor development is the identification and elimination of isolated regions of low J_c that sometimes occur in otherwise high J_c tapes. These “bad” regions limit the end-to-end critical current of the whole tape, even though they may comprise less than 1 % of its length. As there are usually no obvious correlating defects in the substrate, these “bad” regions must occur during the growth and processing of the buffer layers or YBCO film. In order to understand these defective regions, they must first be located with some accuracy along the length of the tape (which also determines their size) and then their structure with respect to current flow should be characterized. This allows the results of further materials analysis techniques to definitively sort out what actually comprises “good” and “bad” materials properties for transport.

Identifying the location and approximate size of bad regions on the tapes has been possible for some time now. This has been demonstrated previously with an instrument that measures J_c at 1 cm intervals along a 100 cm coated conductor tape.¹ Addressing the second requirement, we now also have the ability to observe the current flow pathways in the tapes at 50 micron resolution using a low temperature scanning magnetoresistance microscope. This is described in detail elsewhere² and consists of a mechanism that rasters a magnetoresistive sensor over the surface of a current-carrying tape. Both sensor and sample are immersed in liquid

nitrogen. The area addressed during a single scan is approximately 2 cm square and off-line Fourier transform techniques provide current density maps from the acquired B_z maps.

EXPERIMENTAL

The samples used in this study were 5 cm long sections cut from a single 100 cm long coated conductor tape. The tape was fabricated by depositing 1.5 μm of YBCO (using pulsed laser deposition) on a textured yttria stabilized zirconia (YSZ) layer that had been deposited previously on an Inconel ribbon by ion beam assisted deposition. The whole structure was subsequently sputter coated with 2 μm of silver. This technique is the standard one used in our laboratory for YBCO coated conductor production and is described in detail elsewhere.³ To identify “good” and “bad” sections, the linear 4 point probe J_c map of the tape was obtained and is shown in Figure 1. This was measured in 0.6 T magnetic field to lower the total necessary applied current. We assume that the relative structure is the same in zero applied field. The end-to-end critical current in zero field at 75 Kelvin (liquid nitrogen)⁴ is 70 A, which corresponds to a current density of $\sim 4.5 \times 10^5 \text{ A/cm}^2$.

The sections from segments 6 through 10 on the tape (good) and from segments 48 through 52 (bad) were used in our experiments. The self field distribution of each piece was imaged with transport currents between 5 A and 25 A and the pieces were repositioned within the scanner assembly up to 3 times in order to access $\sim 5 \text{ cm}$ of tape. The actual total image area was slightly less due to the lateral size of the probe. Current density maps were obtained from the B_z maps using standard Fourier transform techniques.⁵

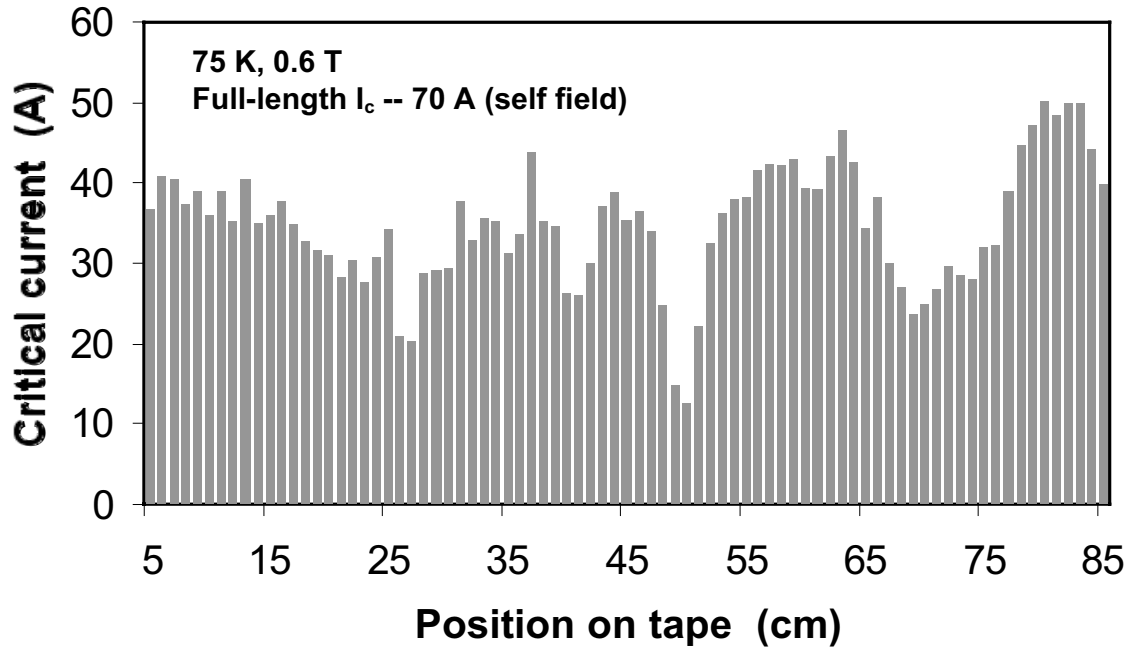


Figure 1. Plot of critical current vs. position on coated conductor tape for the sample in these experiments. The position on the tape can also be referred to as the segment number since the technique has 1 cm resolution.

For the bad tape section, spatially resolved x-ray analysis was also carried out with 1mm resolution. The details of this technique and detailed interpretation of the results are described elsewhere in this proceedings.^{6,7} The general results will be described below and related to the current density pathways.

RESULTS AND DISCUSSION

The current density maps of the good and bad tape sections are shown in Figure 2 for 20 A and 19 A flowing, respectively. All imaging was done with zero applied magnetic field. Horizontal discontinuities in the images are an artifact of joining images acquired from different scans. The good section of tape in Fig. 2a shows the structure expected from our previous studies on test YBCO/Inconel samples and YBCO deposited on single crystal SrTiO₃ – an edge peaked current flow that is very uniform along the tape length.² This structure is consistent with the Critical State Model (CSM) applied to type II superconductors in a thin film geometry.⁸ For this case, demagnetizing effects change the expected current density step function at the sample edges to a distribution that has finite current in the center of the sample and peaks at the edges. In our previous studies of similar samples, increasing the current magnitude leads to growth of the edge peaks and filling in of the middle until the profile is roughly flat at the measured critical current.

The current density map of the bad section of the tape in Fig. 2b immediately clarifies the basic nature of the defect in this region – only half of the tape is carrying an appreciable amount of current. At the top and bottom of the scan the structure appears similar to that of the good section shown in Fig. 2a, but in the middle, near section 50, the current is confined to the right half of the sample. Interestingly, the right half seems to be acting as an independent ribbon of YBCO coated conductor since it maintains a double peaked structure. This indicates an abrupt change in materials properties near the middle of the tape in this region.

The evolution of these current pathways is shown in Figure 3 with grayscale maps and corresponding contour plots from segments 50 and 51. The scan frame has been rotated slightly. The grayscales of each panel have been adjusted individually for ease of viewing and therefore the intensities cannot be compared between panels, only within panels. From these panels, it appears that some current flow is present in the left half at low currents but as the current is increased, the left edge peak moves closer to the center of the tape. From the contour plots it is also obvious that the left edge peak structure is much more non-uniform along the length of the tape than is the right side.

Line profiles of the current density near the upper part of the narrow region are shown in Figure 4 for currents from 10 A to 25 A. These plots show that the current density in the left 40% of the sample has saturated by 10 A. Further increases in the current are accommodated through rightward shifts of the left peak until 20 A is reached and the edge peaked structure occupies the right half of the sample. Beyond this current, the left peak position remains the same and the behavior (growing peaks and filling in the middle) is consistent with that of a good sample. These results also roughly explain the magnitude of the critical current in segment 50 observed in Fig. 1. For example, if there were only good material in half of the tape at segment 50, we would expect $\sim 17 \text{ A} \pm 5 \text{ A}$ critical current based on the 35 A average (in 0.6 T) and the standard deviation in the good sections. The observed $\sim 13 \text{ A}$ falls within the error bars.

Having clearly mapped out the current density pathways in the bad region, spatially resolved x-ray analysis was carried out with 1 mm resolution to correlate materials properties

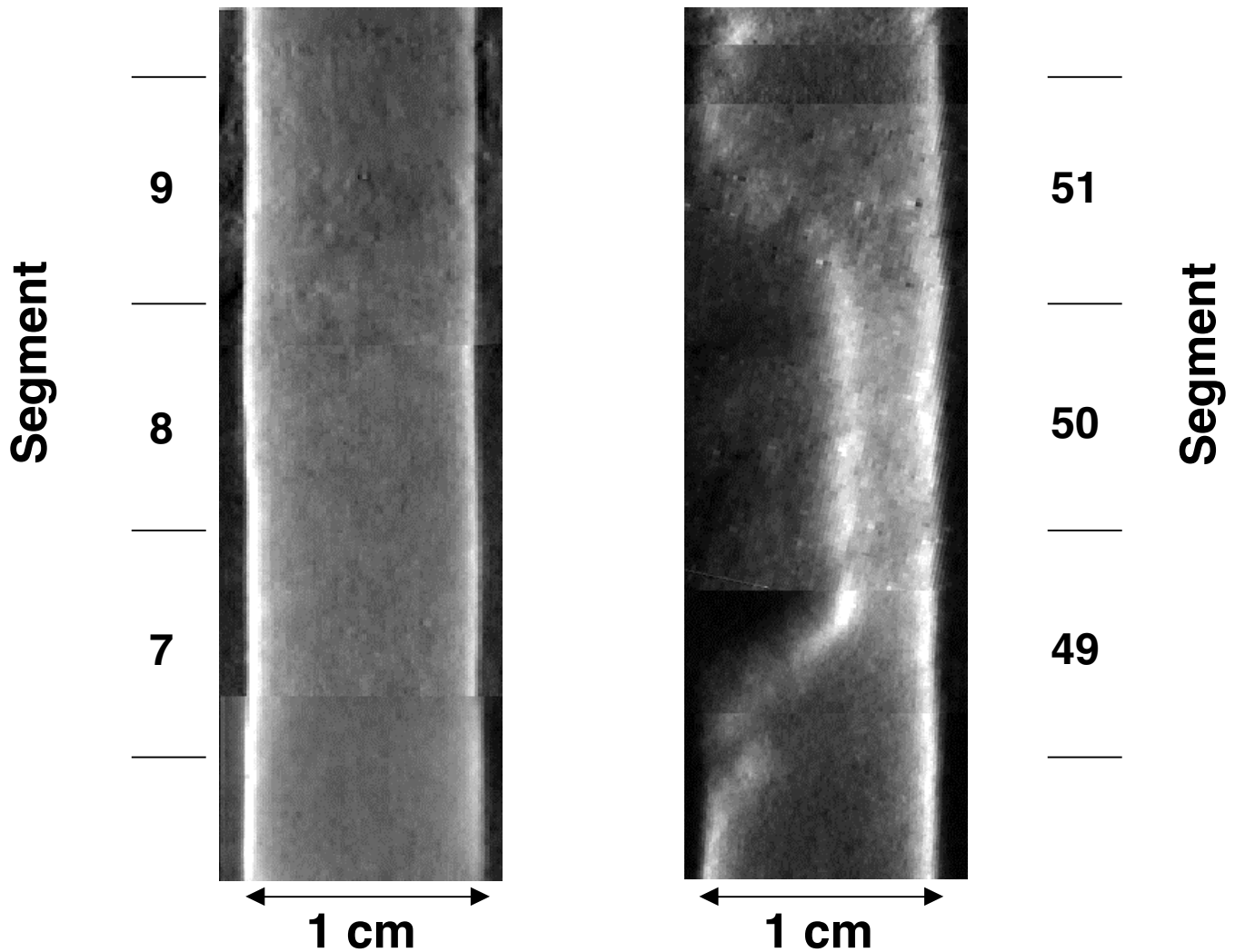


Figure 2. Current density maps along the current flow direction for the a) “good” tape section carrying 20 A and b) “bad” tape section carrying 19 A.

with the observed current distributions. The details and interpretation of the *x*-ray experiments are described elsewhere in this proceedings.^{6,7} They suggest, in part because of increased *a*-axis oriented material in the left side of segment 50, that the substrate temperature was too low in this area during deposition of the YBCO layer. This could occur if misalignment in the deposition system or an irregularity in the Inconel substrate caused that section of the tape to lift off of the heater momentarily. The resulting drop in YBCO deposition temperature for that section could easily explain the increase in *a*-axis material and the low J_c in the “bad” section.

SUMMARY AND CONCLUSIONS

The current maps and *x*-ray data allow us to draw some conclusions about the nature of the defective area. The left half of the bad section is unable to carry current because of poor quality YBCO. However, the flux can move through the left side easily as the current is being

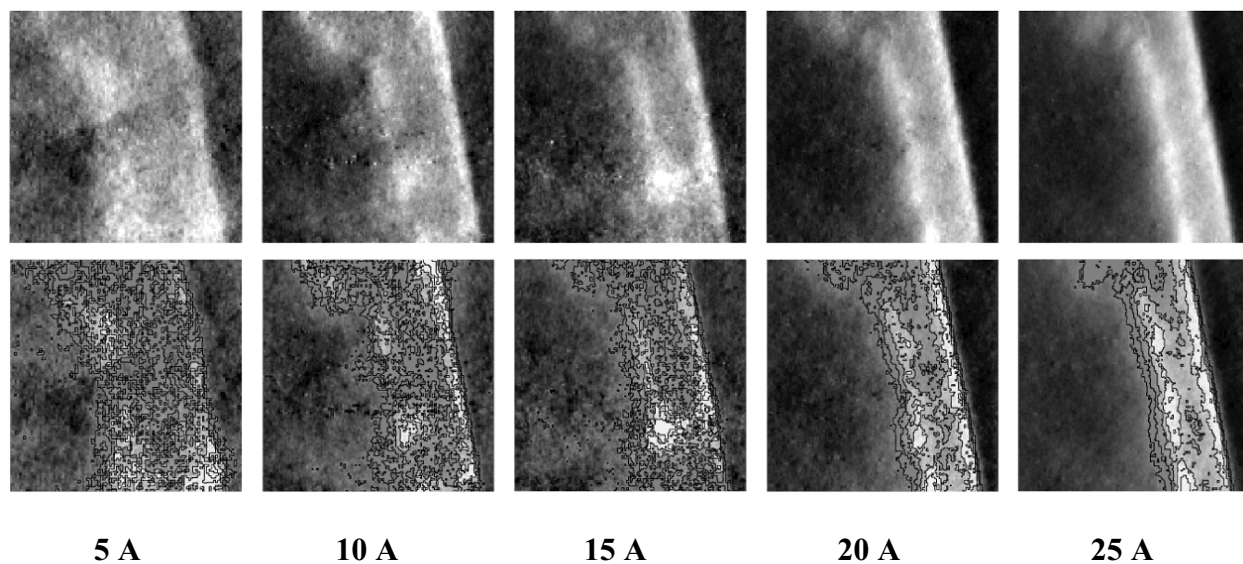


Figure 3. Grayscale current density maps (upper panels) and their corresponding contour plots (lower panels) along the transport current direction for the currents labeled at the bottom. Image areas are ~ 1.75 cm x 1.75 cm.

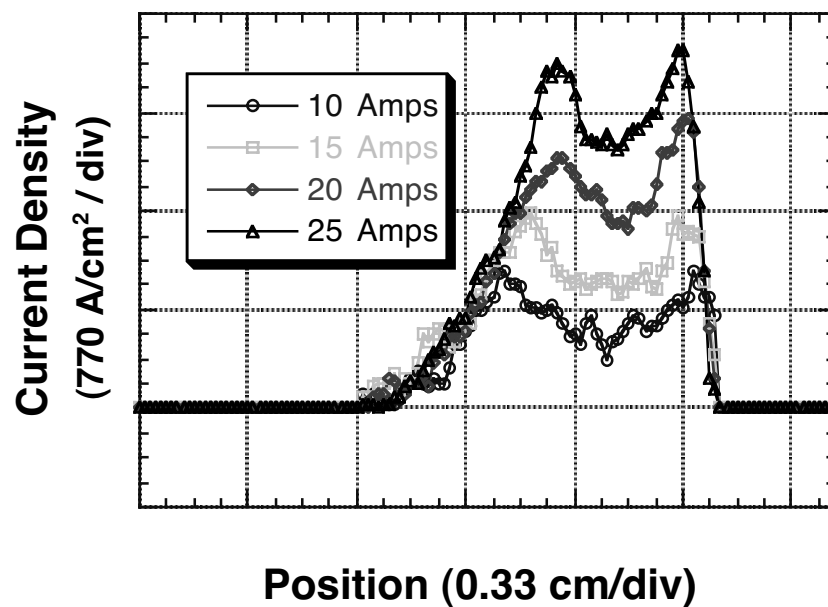


Figure 4. Current density profiles from the upper part of segment 50.

increased, perhaps through a network of weak links. At constant transport current, the double peaked structure on the right side is produced because the flux front has reached the material with good properties (i.e. a large number of strong pinning sites). This is consistent with the x -ray results showing large a -axis (low c -axis) density on the left side of the tape and low a -axis (large c -axis) density on the right side of the tape.

In summary, we have imaged the current transport pathways in good and bad sections of a 1-cm-wide YBCO coated conductor and have been able to correlate degraded transport properties with increased a -axis material density. These results are promising since they demonstrate an effective technique for understanding similar defects. Further studies, already in progress, will help determine if other low J_c regions have similar properties. These results will help suggest possible changes in the processing technique to eliminate these defects.

We thank M. Maley for useful discussions on superconductivity and flux flow in YBCO. This work was supported by the United States Department of Energy - Office of Energy Efficiency and Renewable Energy.

¹ S.R. Foltyn, et. al., *Physica C* **341-348**, 2305 (2000).

² G.W. Brown, et. al., *to appear in High-Temperature Superconductors – Crystal Chemistry, Processing and Properties*, edited by U. Balachandran, H.C. Freyhardt, T. Izumi, and D.C. Larbalestier (Mat. Res. Soc. Proc. **659**, Pittsburgh, PA, 2001) p II7.4.

³ S.R. Foltyn, et. al., *IEEE Trans. Appl. Supercond.* **9**, 1519 (1999).

⁴ 75 K is the boiling point of liquid nitrogen at the altitude of our laboratory in Los Alamos, NM USA.

⁵ B.J. Roth, N.G. Sepulveda, and J.P. Wikswo, Jr., *J. Appl. Phys.* **65**, 361 (1989).

⁶ E.J. Peterson, et. al., *This Proceedings*.

⁷ F.M. Mueller, et. al., *This Proceedings*.

⁸ E. Zeldov, J.R. Clem, M. McElfresh, and M. Darwin, *Phys. Rev. B* **49**, 9802 (1994).